Gap-states distribution of ion-implanted Si and GaAs from subgap absorption measurements

U. Zammit, M. Marinelli, R. Pizzoferrato, and F. Mercuri
Dipartimento Ingegneria Meccanica, II Università di Rome "Tor Vergata," Via della Ricerca Scientifica, 00173 Roma, Italy
(Received 12 December 1991)

The distribution of gap states has been obtained from subgap absorption measurements in ion-implanted Si and GaAs layers and the changes induced by increasing the implantation ion dose have been monitored. The variations in slope which are observed with increasing dose in the spectral region at energies lower than the band-edge region are shown to be mainly affected by a shift of the energy position of the peak of the calculated distributions.

INTRODUCTION

Gap states in disordered and amorphous semiconductors directly affect their optical and electron transport properties. It is therefore most important to study the energy distribution of such states which originate from absence of long-range order, and also from dangling bonds, defects, and impurities present in the material. Extensive work has been carried out in this respect on hydrogenated amorphous silicon (*a*-Si:H) using a variety of experimental techniques such as electron spin resonance, luminescence, optical absorption, photoconductivity, and conductivity measurements.[1,2] Recently, a detailed analysis of the gap density-of-states results obtained from optical absorption measurements and carried out in intrinsic and doped *a*-Si:H has been presented.[3] The results have been interpreted in terms of the enegy position and of the width of a peaked distribution of gap states caused by uncharged and charged dangling bonds and impurities and have been found to be in good agreement with the ones obtained previously with optical absorption measurements as well as with other techniques.[3]

Very little has so far been reported on the gap-states distribution associated with implantation damage in ion-implanted semiconductors despite their extensive technological applications for integrated optics and electronics. Subgap absorption measurements have already been reported for implanted layers of GaAs (Refs. 4 and 5) and Si,[5] as a function of implantation temperature, ion dose, and energy, but only empirical and/or qualitative conclusions could be drawn. Qualitatively similar results have been found in the two kinds of semiconductors despite the greater variety and complexity of defects which arise during implantation of compound semiconductors with respect to elemental ones. In particular, two distinct regions have been observed in the absorption spectra, one corresponding to the band-edge region and the second one found at lower energies, both exhibiting an exponential behavior but with strongly different values of the logarithmic slope. Moreover, the value of such a quantity found in the lower-energy region was observed to decrease for increasing implantation doses, so long as the implanted layer consisted of damaged crystalline material, while further doses increases, which caused the implanted layer to turn partially or completely amorphous, induced an increase and a saturation of the value.

In this work we report on the gap-states energy distribution obtained for ion-implanted Si and GaAs layers from subgap absorption measurements. Due to the great variety and complexity of the defects arising from the implantation process, it will not be possible, from the present optical absorption measurements alone, to ascribe any given gap-states distribution to a particular kind of defects, unlike the case of *a*-Si:H where the distributions have been ascribed to uncharged and charged dangling bonds and impurities. Nonetheless, changes occurring in the distribution of the gap states, as a function of the implantation dose, will be monitored.

RESULTS AND DISCUSSION

The optical absorption data have been obtained by photothermal deflection spectroscopy measurements. The experimental setup, as well as the theoretical expressions adopted to obtain the absorption spectra of the implanted layer alone, are reported in Ref. 6. The measurements have been performed on Si samples implanted at room temperature with 100-keV Si ions and with 150-keV P ions and on GaAs samples implanted at room temperature with 100-keV Si ions. Figure 1 shows the absorption spectra obtained for the GaAs implanted layers. The two distinct spectral regions exhibiting a practically linear behavior on the semilog plot, and therefore the exponential energy dependence mentioned earlier on, are clearly evident in the spectra. Besides a progressive increase in the absorption values found with increasing implantation dose, it is shown that the slopes of the lower-energy region data curves progressively decrease for implantation dose increase up to the value of 10^{14} cm^{-2}. For larger doses, corresponding to which electron diffraction analysis showed formation of amorphous material in the implanted layer, the slope shows a substantial increase. It is also interesting to note that the spectral region characterized by the smaller slope extends, with increasing ion dose, towards higher energies, at the expense of the larger slope region which, for the largest doses, can hardly be detected over the spectral region covered by the present data. It is not, on the other hand, possible to extend the investigations to higher energies because of the very strong absorption of the crystalline substrate which is typically 10^3 times thicker than the implanter

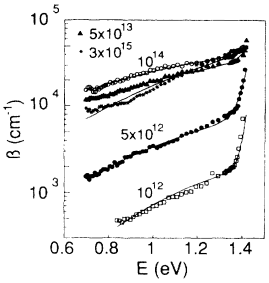

FIG. 1. Subgap absorption spectra for GaAs samples implanted with various doses of 100-keV Si ions. The continuous lines represent the convolution integral fit results.

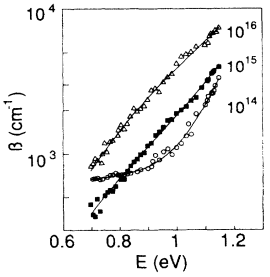

FIG. 3. Subgap absorption spectra for Si samples implanted with various doses of 150-keV P ions. The continuous lines represent the convolution integral fit results.

layer. The results for ion-implanted Si are reported in Figs. 2 and 3. Though with respect to GaAs a smaller range of implantation doses below the amorphization threshold is reported, even in the case of Si it is shown that the value of the slope of the data curves in the region below the band edge increases when the implanted layer becomes amorphous. Also, the spectral region characterized by the smaller slope once again extends, with increasing ion dose, towards higher energies, at the expense of the larger slope region. The results are also shown to be independent of the implanted species. The results for the Si and GaAs implanted layers are summarized in Fig. 4 where the lower-energy region logarithmic slope K ($\beta=\beta_0 e^{KE}$, β is the absorption coefficient and E is the photon energy), is reported as a function of $\bar{G}_n$, the mean energy per unit volume deposited by nuclear collision by the implanted ions. $\bar{G}_n=\bar{E}\Phi/d$, where $\bar{E}$ is the mean energy per unit length deposited by the implanted ions, Φ is the implantation dose, and d is the thickness of the implanted layer. $\bar{E}$ and d were calculated by means of a code for the simulation of particle penetration in amorphous solids (TRIM Monte Carlo code[7]). Some of the data shown in Fig. 4 correspond to spectra now shown in the previous figures and the values relative to implanted Si have been shifted vertically by 2 eV^{-1}. For both kinds of semiconductors, the values of K initially decrease with increasing $\bar{G}_n$ and then increase and saturate once values of $\bar{G}_n$ are reached corresponding to which amorphous material forms in the implanted layer. The dotted lines in the present and following figures represent a guide to the eye.

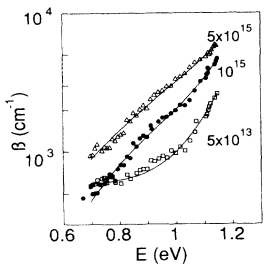

FIG. 2. Subgap absorption spectra for Si samples implanted with various doses of 100-keV Si ions. The continuous lines represent the convolution integral fit results.

The subgap optical absorption spectra reflect the convolution of the initial and final densities of states between which the electronic transitions occur. The interpretation of the optical absorption spectra is thus quite complex and requires certain assumptions in order to derive information about the enegy distribution of the gap states. In accordance with earlier work, carried out on a:Si-H,[3,8,9] to interpret the subgap absorption spectra we consider only transitions from occupied localized states above the valence-band edge E_v to unoccupied extended states above the conduction band edge E_c. We neglect transitions from extended valence-band states to conduction-band tail states implying that the conduction-band edge is sufficiently steep. This has been verified for a:Si-H (Ref. 10) as well as for heavily doped crystalline GaAs.[11] Furthermore we assume that the optical matrix element for transitions from localized to extended states is constant with respect to the photon energy[12] and that the one from localized to localized states is negligible. We consider the localized states consisting of an exponential valence-band tail distribution and a peaked distribution of gap states.[3,8]. Though, in fact, it has been shown that an exponential distribution of gap states combined with cutoff at the Fermi energy gave comparatively good fit for undoped a:Si-H,[9] the same would not hold for highly doped a:Si-H.[3] A Gaussian distribution of gap states, on the other hand, has led to results in agreement with ones obtained with other than optical techniques in both undoped and doped a:Si-H.[3]

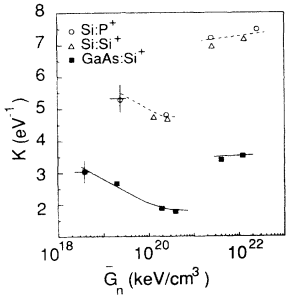

FIG. 4. Logarithmic slope K of the lower-energy region of the absorption spectra of ion-implanted GaAs and Si layers as a function of the ion mean nuclear deposited energy density $\bar{G}_n$. Values for implanted Si have been shifted vertically by 2 eV^{-1}. The lines represent a guide to the eye.

Considering a parabolic distribution of conduction-band states, the optical absorption is finally given by

$$\beta=\frac{R}{E}\int \varepsilon^{1/2}\left\{N_v\exp\left[-\frac{(\varepsilon+E_g-E)}{E_0}\right]+N_r\exp\left[-\frac{(\varepsilon+E_r-E)^2}{E_w^2}\right]\right\}d\varepsilon ,$$

where R is a constant; E is the photon energy; ε is the energy coordinate measured from E_c; N_v and E_0 are, respectively, the valence-band tail density of states at E_v and the inverse logarithmic slope; E_g is the band gap; N_r is the density of states at the peak of gap-states Gaussian distribution, E_r the distance of its peak from E_c and $2E_w$ its width. We assume for ion-implanted material the same value of E_g as for the crystalline one since we have found that the energy position of the fundamental band edge in the spectra of the two kinds of materials is the same.[5] The fitting parameters of the convolution integral in the present work were E_r, E_w, N_v/N_r, and E_0. The results of the fitting procedure are represented by the continuous lines in Figs. 1–3. Figure 5 shows the changes which are observed in the gap-states distribution parameters for increasing implantation does in the case of implanted GaAs. Corresponding to the initial decrease of the logarithmic slope and the subsequent increase, shown in Fig. 4, the position of the peak first tends to shift away from the valence-band edge and then moves considerably towards it once the implanted layer turns amorphous. The position of the peak strongly affects the slope of the absorption data curve since, for example, the shift away from the valence-band edge would enhance lower-energy transitions with respect to larger-energy ones, thus reducing the slope of the curve (and vice versa). Regarding the width of the distribution, after a slight initial increase, which would also act towards a decrease of the slope of the curve, there is no further substantial change which could significantly change the slope of the curves. It thus seems that it is the peak position which mainly affects the slopes of the curves. The results for ion-implanted Si are shown in Fig. 6 and, as expected, are qualitatively very similar to those of GaAs. The changes which are induced with varying implantation does in the

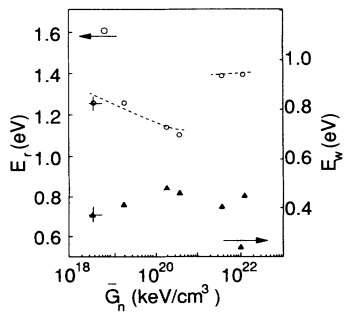

FIG. 5. Gap-states distribution peak position E_r and half-width E_w as a function of $\bar{G}_n$ for ion-implanted GaAs. The dotted line represents a guide for the eye.

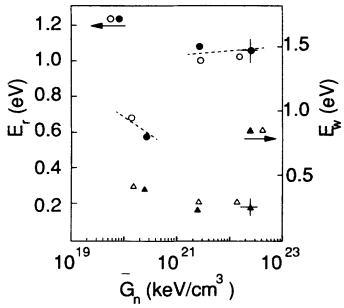

FIG. 6. Gap-states distribution peak position E_r and half-width E_w as a function of $\bar{G}_n$ for Si implanted with Si ions (open symbols) and P ions (filled symbols). The dotted line represents a guide to the eye.

gap-states distributions are due to the changes in variety and complexity as well as overall number of defects which are formed in the implanted material when the ion dose is increased. Figure 7 finally shows the ratio N_r/N_v vs $\bar{G}_n$. Its increase reflects the increase of the subgap absorption values with implantation dose which is caused by the increased number of induced defects.

We can now compare the results obtained for amorphous Si (a:Si) obtained by ion implantation to those relative to a:Si-H. Apart from the strongly different optical gap values (≈ 1.7 eV for a:Si-H), the subgap absorption values found in implanted a:Si are much larger than the ones found in a:Si-H. This is reflected in a considerably larger value of N_r/N_v found in implanted a:Si [$N_r/N_v \approx 5\times 10^{-3}$ in heavily P-doped a:Si-H (Ref. 8)]. Both the subgap absorption values and the optical gap value in implanted a:Si are much closer to those of evaporated a:Si [$E_g \approx 1.23$ eV (Ref. 13)]. This is due to the absence of Si-H bonds in implanted and evaporated a:Si.

Another difference which appears between the absorption spectra of a:Si-H and implanted a:Si is that in the former case, below the fundamental band-edge region, the data show shoulder-shaped profile characterized by an initial smooth decrease, with decreasing photon energy, followed by a steeper decrease about 0.2–0.4 eV below the band edge, in contrast with the latter case where the data show a uniform decrease with decreasing energy below the band-edge region. This is also true for

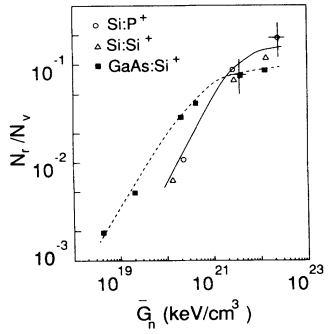

FIG. 7. N_r/N_v (see text) vs $\bar{G}_n$ for ion-implanted GaAs and Si layers. The lines represent a guide to the eye.

implanted a:GaAs. The data profile observed in a:Si-H is well accounted for by a distribution of gap states characterized by a peak position about 1 eV below E_c and a half-width $E_w = 0.1$ eV. The uniform slope profile obtained in the case of implanted a:Si is accounted for by a peak position which is also about 1 eV below E_c but by a considerably larger width ($E_w = 0.25-0.3$ eV).

CONCLUSIONS

We have calculated the energy distribution of gap states induced by the ion implantation process in Si and GaAs from subgap absorption measurements. Two distinct regions have been observed in the absorption spectra, one corresponding to the band-edge region and the second one found at lower energies, both exhibiting a practically exponential energy dependence but with different values of the logarithmic slope. The same trend has been found, for Si and GaAs, in the implantation dose dependence of the lower-energy region values of the logarithmic slope which was observed to increase for increasing implantation dose when the implanted layer consisted of damaged crystalline material, while further dose increase, which caused amorphous material to form in the implanted layer, induced a decrease in the value. The absorption spectra have been interpreted in terms of a peaked distribution of gap states. It has been shown that it is mainly the energy position of the peak of the distribution, rather than its width, that affects the lower-energy slope of the absorption spectra. As the implantation dose increases, the peak position is first observed to shift away from the valence-band edge, but it tends to shift considerably towards the valence-band edge when amorphous material forms in the implanted layer.

[1]H. Fritzsche, J. Non-Cryst. Solids **77/78**, 273 (1985).

[2]R. A. Street and D. K. Biegelsen, in *The Physics of Hydrogenated Amorphous Silicon II,* edited by J. D. Joannopulos and G. Lucovsky (Springer-Verlag, Berlin, 1984).

[3]A. Triska, J. A. Kocka, and M. Vanecek, in *Disordered Semiconductors,* edited by M. Kastner, G. A. Thomas, and S. R. Ovshinsky (Plenum, New York, 1987), p. 459, and references therein.

[4]E. Wendler, W. Wesch, and G. Götz, Phys. Status Solidi A **93**, 207 (1986); W. Wesch, E. Wendler, and G. Götz, Nucl. Instrum. Methods B **22**, 532 (1987).

[5]U. Zammit, F. Gasparrini, M. Marinelli, R. Pizzoferrato, A. Agostini, and F. Mercuri, J. Appl. Phys. **70**, 7060 (1991).

[6]U. Zammit, M. Marinelli, and R. Pizzoferrato, J. Appl. Phys. **69**, 3286 (1991).

[7]J. P. Biersack and L. G. Haggmark, Nucl. Instrum. Methods **174**, 257 (1980).

[8]C. R. Wronsky, B. Abeles, T. Tiedje, and G. D. Cody, Solid State Commun. **44**, 1423 (1982); W. B. Jackson and N. B. Amer, J. Phys. (Paris) Colloq. **42**, C4-293 (1981); Bull. Am. Phys. Soc. **27**, 230 (1982).

[9]J. S. Payson and S. Guha, Phys. Rev. B **32**, 1326 (1985).

[10]T. Tiedje, J. M. Cebulka, D. L. Morel, and B. A. Abeles, Phys. Rev. Lett. **46**, 1425 (1981).

[11]J. I. Pankove, Phys. Rev. **140**, A2059 (1965).

[12]W. B. Jackson, S. M. Kelso, C. C. Tsai, J. W. Allen, and S. J. Oh, Phys. Rev. B **31**, 5187 (1985).

[13]N. F. Mott and E. A. Davies, *Electornic Processes in Noncrystalline Materials* (Clarendon, Oxford, 1979), pp. 384–388.